J Electr Eng Technol.2018; 13(4): 1450-1458
http://doi.org/10.5370/JEET.2018.13.4.1450

ISSN(Print) 1975-0102
ISSN(Online) 2093-7423

Design of Direct-Current Fuzzy Controller for Mitigating Commutation Failure in HVDC System

Benfeng Gao*, Kewei Yuan†, Peiyi Dong, Chao Luo*** and Shuqiang Zhao***

Abstract – Commutation failures can deteriorate the availability of high-voltage direct current (HVDC) links and may lead to outage of the HVDC system. Most commutation failures are caused by voltage reduction due to ac system faults on inverter side. The commutation failure process can be divided into two stages. The first stage, from the occurrence to the clearing of faults, is called '*Deterioration Stage*'. The second stage, from the faults clearing to restoring the power system stability, is called '*Recovery Stage*'. Based on the analysis of the commutation failure process, this paper proposes a direct-current fuzzy controller including prevention and recovery controller. The prevention controller reduces the direct current to prevent Commutation failures in the '*Deterioration Stage*' according to the variation of ac voltage. The recovery controller magnifies the direct current to speed up the recovery of power system in the '*Recovery Stage*', based on the recovery of direct voltage. The validity of this proposed fuzzy controller is further proved by simulation with CIGRE HVDC benchmark model in PSCAD/EMTDC. The results show the commutation failures can be mitigated by the proposed direct-current fuzzy controller.

Keywords: HVDC, Commutation failure, Fuzzy controller, PSCAD/EMTDC, CIGRE

1. Introduction

High-voltage direct current (HVDC) based on line-commutated converter is widely used in power networks with long distances. According to real experience, commutation failure is one of the most frequent inverter failures in the HVDC systems [1-3]. Most commutation failures are caused by transient faults on the inverter side.

A commutation failure can severely threaten power system stability [4-6]. For example, it can result in significant increase of direct current and shorten the lifespan of converter valves which will cause a security risk [7]. In addition, commutation failures give rise to temporary interruption of transmitted power or even lead to power outage. Occasionally, a commutation failure can trigger serious transients such as system resonances leading to longer duration power curtailments and even severe cascading failures. From this perspective, commutation failure frequency can be used as an index of unavailability of HVDC links [8, 9]. Thus, further analysis on commutation failure and corresponding measures to reduce the aforementioned effect are of significant importance.

Various research on reducing the risk of Commutation failures have been reported in the literature. To handle these problems, various methods have been developed based on the analysis mechanism of commutation failures [10-13]. The authors in [10] put forward a method to directly detect the deionization margin angle and to prevent the commutation failure of an inverter. The authors in [11] propose a DC control strategy based on an idea of sine-cosine components detector. The controller quickly predicts a necessary control angle through the control strategy to make the power system recover better from commutation failures. The [12] employs fuzzy logic controller to improve the performance of the HVDC systems under various faults and operating point changes. The [13] proposes an approach to design a fuzzy-PI controller based on Genetic Algorithms in the HVDC system. However, these works neglect the difference between different stages of commutation failure. Only one control strategy is used throughout the process of commutation failure.

The process of commutation failure can be divided into two stages. The first stage is from the occurrence to the clearing of faults. In this stage, the ac bus voltage reduces and the direct current increases rapidly. The extinction angle in the inverter side system decreases at first and then increases again. This stage is defined as '*Deterioration Stage*'. The second stage is from the faults clearing to restoring the power system stability. The ac bus voltage begins to recover in this stage. The direct current and the extinction angle also begin to return to the rated value. The second stage is defined as '*Recovery Stage*'.

The contributions of this paper are shown as below. (1) The process of commutation failure is divided into

† Corresponding Author: Department of Electrical Engineering, North China Electric Power University, China. (keweiyuan_ncepu@163.com)
* Department of Electronic Engineering, North China Electric Power University, China. (gaobenfeng@126.com, zsqdl@163.com)
** State Grid Baoding Electric Power Supply Company, China. (dongpeiyi123@163.com)
*** Electric Power Research Institute of China Southern Power Grid, China. (ceeelch@126.com)
Received: August 1, 2017; Accepted: February 11, 2018

two stages: '*Deterioration Stage*' and '*Recovery Stage*'. The characteristics of two stages are analyzed in detail. (2) Based on the above analysis, a direct-current fuzzy controllers is proposed, which includes prevention controller for '*Deterioration Stage*' and recovery controller for '*Recovery Stage*'. The prevention controller reduces the direct current to prevent the commutation failure in the '*Deterioration Stage*' according to the variation of ac voltage. The recovery controller magnifies the direct current to speed up the recovery of power system in the '*Recovery Stage*'. (3) The inputs, structure, and realization of the proposed controllers is introduced. The proposed direct-current fuzzy controller can not only decrease the frequency of Commutation failures but also speed up the recovery of the system from ac faults. It provides an effective method for mitigation of commutation failures in the HVDC systems.

The rest of this paper is organized as follows. In Section 2, the test system and control system in CIGRE HVDC benchmark model are given. Section 3 explores the analysis of commutation failures and structure of direct-current fuzzy controller. Section 4 shows the process of determining the input variables. Section 5 introduces the design of the direct-current fuzzy controller. The simulation results are given in Section 6. Section 7 draws the conclusion.

2. Test System

The CIGRE HVDC benchmark model has been used here as the test system to design the direct-current fuzzy controller. The HVDC system, shown in Fig. 1, is a mono-polar 1000-MW HVDC link with 12-pulse converters on both rectifier and inverter sides. The inverter side is connected to the weak ac system, which has a short circuit ratio of 2.5 at 50 Hz. Damped filters and capacitive reactive compensation are also provided on both sides to supply the reactive power. The rated voltage of the rectifier side ac system is 345 kV, while that of the inverter side is 230 kV. The direct voltage is maintained as a constant with the reference voltage being 500 kV [14]. The control model mainly includes the measurement of electrical parameters and the generation of the trigger signals of the rectifier and the inverter. The block diagram of the controller is shown

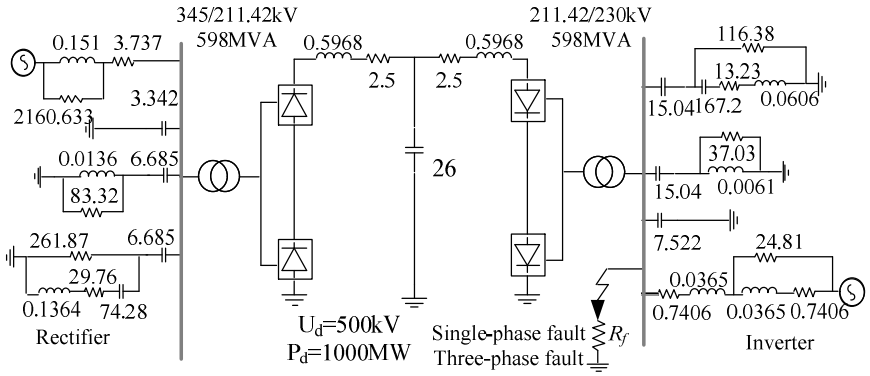

Fig. 1. Simulation model

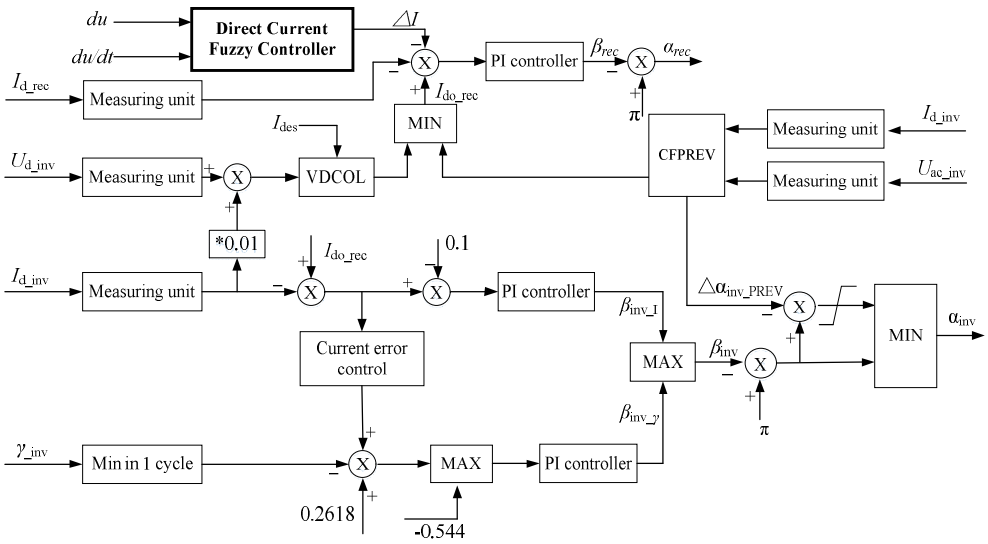

Fig. 2. Block diagram of controllers in the CIGRE HVDC benchmark model

in Fig. 2.

In general, the control of HVDC power is realized by the coordinated adjustment of direct current on rectifier side and direct voltage on inverter side. In Fig. 2, under normal conditions, the rectifier side operates under constant current control to control the direct current, and the inverter side usually operates under constant extinction angle control to regulate the direct voltage.

The rectifier side is equipped with constant current controller to maintain the direct current constant. The reference value of direct current, denoted as $I_{\mathrm{do\_rec}}$, is obtained from dependent current order limiter (VDCOL) at the inverter side. The direct current at the rectifier side, denoted as $I_{\mathrm{d\_rec}}$, is measured using measuring unit which contains necessary filters. The reference and measured value of direct current is compared, and an error signal is generated. This error signal is fed to PI controller to produce the next firing angle order α_{rec} for the valve of rectifier side.

The extinction angle control and constant current control are implemented on the inverter side. The measured value of extinction angle $\gamma_{\mathrm{\_inv}}$ is compared with the reference value of extinction angle. The error signal is fed to PI controller which generate the firing angle order $\beta_{\mathrm{inv\_}\gamma}$. The constant current control at inverter side is similar to the rectifier current controller. The measured current $I_{\mathrm{d\_inv}}$ is subtracted from the reference value to produce an error signal, and then is sent to the PI controller to generate the required angle order $\beta_{\mathrm{inv\_I}}$. The outputs of two controllers, $\beta_{\mathrm{inv\_}\gamma}$ and $\beta_{\mathrm{inv\_I}}$, are compared, and the maximum β_{inv} is used to produce the firing angle order for valve of inverter side. Under normal conditions, the inverter side operates under constant extinction angle control. The detailed information about the controllers in Fig. 2 can be found in [15]

In Fig. 2, the function CFPREV (commutation failure prevention) is added at the inverter side to reduce the commutation failures caused by ac faults. When detecting ac faults, this function outputs an additional angle $\triangle\alpha_{\mathrm{inv\_PREV}}$ to enlarge the commutation margin and reduce the risk of commutation failures. The details about CFPREV is introduced in [16].

3. Design Principle of Direct-Current Fuzzy Controller

3.1 Analysis of the commutation failures process

Commutation failures following ac system disturbances may occur in HVDC systems [17]. As mentioned above, the process of commutation failure is divided into two time stages, defined as '*Deterioration Stage*' and '*Recovery Stage*'.

During the '*Deterioration Stage*', the magnitude of ac voltage reduces and the direct voltage modulated by ac voltage also decreases. The direct current increases dynamically [18]. The commutation margin is affected by voltage magnitude reduction, increased overlap due to higher direct current and phase angle shifts. In this stage, decreasing the direct current command can slow down the deterioration of the system.

The process is different in the '*Recovery Stage*'. The direct voltage increases with the recovery of the ac voltage. The direct current returns to the reference value. The commutation margin begins to revert to the rated value. The system then gradually returns to stability. At this point, increasing the direct current command is beneficial for power recovery.

Because of the preceding differences, it is necessary to design corresponding fuzzy controllers for different stages. These fuzzy controllers can mitigate the effect of commutation failures at different stages.

3.2 Structure of direct-current fuzzy controller

Based on the analysis, mentioned above, this paper proposes a novel direct-current fuzzy controller to mitigate commutation failures. It consists of two parts: prevention controller and recovery controller, as shown in Fig. 3.

These two fuzzy controllers act on different stages of the commutation failure process. The prevention controller is designed for '*Deterioration Stage*'. According to the ac voltage, the prevention controller will reduce the direct current command to retard the commutation failure. The

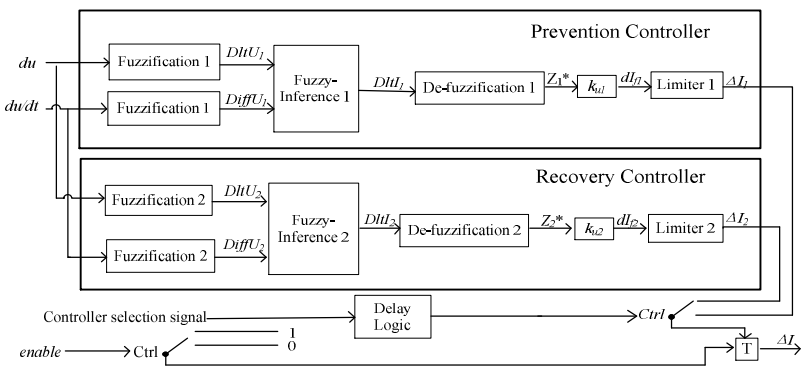

Fig. 3. Schematic diagram of the direct-current fuzzy controller

recovery controller is designed for '*Recovery Stage*'. It will increase direct current command to speed up the restoration of the HVDC system.

du and *du/dt* are the inputs of the current fuzzy controller (the determination process is given in Section 4.). Based on their levels, the direct current correction, denoted by ΔI, is calculated following fuzzy control theory. ΔI is the output of the fuzzy controller and is superimposed on the constant current control (Fig. 2).

The two fuzzy controllers are switched by the controller selection signal '*Ctrl*'. The default initial state of the controller selection is the prevention controller. During the commutation failure, the ac bus voltage is monitored by measuring *du* and *du/dt*. When the ac voltage begins to recover, the output will be switched from the prevention controller to recovery controller.

The direct-current fuzzy controller can only be enabled after an ac system fault is detected. Thus, the signal defined as '*enabled*' is essential to control the input and removal of fuzzy controller. Each time an ac fault occurs, the '*enable*' signal is set to '1'. The direct-current fuzzy controller is put in and the prevention controller is selected. After the HVDC system is stabilized, the '*enable*' is set to '0', and the direct-current fuzzy controller is removed.

4. Inputs of Direct-Current Fuzzy Controller

The selection of the fuzzy controller input signal directly affects its control effect. For the direct-current fuzzy control proposed in this study, the inputs should be the most affecting factors as to the onset of commutation failures. The prevention controller and recovery controller have similar design processes. In the following study, the prevention controller is used as an example to demonstrate the design process.

The vast majority of commutation failures are caused by the failure of the ac system. Therefore, these key factors can be identified by simulations of single-phase and three-phase ac system faults on the basis of the HVDC test system as shown in Fig. 1.

4.1 Study of single-phase ac system faults at the inverter

A single-phase to ground fault is applied at t =0.1 s with a duration of 100 ms. A fault resistance, denoted by R_f, is connected at the fault location as shown in Fig. 1. By varying R_f between 0 Ω and 260 Ω in steps of 20 Ω, single-phase test results are shown in Table 1.

Where, *du* denotes the ac bus voltage reduction, *du/dt* refers to the rate of change of the ac bus voltage, β_{min} refers to the minimum of extinction angle, and I_{dMAX} denotes the maximum direct current. R_f is the fault resistance and can also indicate the severity of the fault. CF is the commutation failure signal, where a value '1' indicates the occurrence of commutation failures and '0' indicates that no commutation failure has occurred.

According to Table 1, the commutation failure first occurs when R_f decreases to 120 Ω. With the decrease of R_f, *du*, *du/dt* and I_{dMAX} becomes larger, whereas $\beta_{\min}$ gradually reduces. When the commutation failure occurs, $\beta_{\min}$ becomes zero. It can be seen that for CF equal to '1', *du* and *du/dt* values are larger than the ones when CF is equal to '0'.

It should also be noticed that I_{dMAX} values in the cases of R_f decreasing from 120 Ω to 60 Ω are almost the same. I_{dMAX} is not sensitive enough to reflect the status of the system explicitly.

Therefore, a conclusion can be drawn that *du* and *du/dt* jointly decide whether a commutation failure has occurred or not.

4.2 Study of three-phase ac system faults at the inverter

The three-phase to ground fault is applied at t =0.1 s with a duration of 100 ms. The fault resistance R_f varies

Table 1. Statistics of single-phase faults

R_f (Ω)	du (p.u)	du/dt (p.u)	β_{min} (°)	CF	I_{dMAX} (kA)
0	0.1400	0.0350	0	1	2.45
20	0.0600	0.0160	0	1	2.48
40	0.0440	0.0110	0	1	2.02
60	0.0360	0.0090	0	1	2.00
80	0.0290	0.0080	0	1	1.99
100	0.0260	0.0070	0	1	1.98
120	0.0250	0.0068	0	1	1.99
140	0.0240	0.0060	6.05	0	1.20
160	0.0240	0.0055	7.76	0	1.17
180	0.0220	0.0053	8.80	0	1.15
200	0.0200	0.0048	9.58	0	1.13
220	0.0190	0.0046	10.18	0	1.12
240	0.0187	0.0043	10.68	0	1.11
260	0.0180	0.0041	11.08	0	1.10

Table 2. Statistics of three-phase faults

R_f (Ω)	*du* (p.u)	*du/dt* (p.u)	β_{min} (°)	CF	I_{dMAX} (kA)
0	0.1500	0.0490	0	1	2.59
20	0.1100	0.0300	0	1	2.56
40	0.0630	0.0220	0	1	2.52
60	0.0500	0.0140	0	1	2.52
80	0.0450	0.0110	0	1	2.50
100	0.0410	0.0100	0	1	2.02
120	0.0395	0.0100	0	1	2.03
140	0.0390	0.0120	0	1	2.60
160	0.0367	0.0090	0	1	2.02
180	0.0361	0.0090	0	1	2.02
200	0.0350	0.0130	0	1	2.00
220	0.0297	0.0050	7.50	0	1.19
240	0.0270	0.0045	8.10	0	1.18
260	0.0247	0.0040	8.90	0	1.17
280	0.0240	0.0034	9.60	0	1.15
300	0.0230	0.0030	10.10	0	1.14
320	0.0210	0.0024	10.54	0	1.15

from 0 Ω to 320 Ω in steps of 20 Ω. Similar simulations are conducted based on the test system. The results are shown in Table 2.

According to Table 2, *du*, *du/dt,* and I_{dMAX} increase with the decrease of R_f. The commutation failure first occurs when R_f decreases to 200 Ω. $\beta_{\min}$ gradually decreases and vanishes for the condition of CF equal to '0'. The trend for each electrical variable is the same as in single-phase ac fault conditions.

As can be seen from the above results, the variables *du* and *du/dt* are sensitive to commutation failure and can reflect the severity of the fault. Therefore, it can be confirmed that du and *du/dt* are the inputs of the direct-current fuzzy controller.

5. Introduction to the Fuzzy Control Mechanism

The proposed fuzzy controller includes three steps: fuzzification, fuzzy-inference, and defuzzification [19, 20]. In this section, the prevention controller is used as an example to demonstrate the design process.

5.1 Fuzzification and fuzzy-inference

In practical systems, fuzzy variable representation is more accurate than exact variable and also provides more information. Fuzzification is the process of converting crisp input variables into fuzzy variables.

According to the simulation results in Section 4, considering a certain margin, the critical range of *du* where the commutation failure of the direct current system occurs is determined as [0.025, 0.030]. Similarly, the complete range of *du/dt* used for the simulation is [-0.05, 0.05], and the critical range for the commutation failure is [0.005, 0.01].

The current values of *du* and *du/dt* are converted into discrete numeric values. For instance, the range of the input variable is [-*a*, *a*] and range of the discrete numeric value is [-*m*, *m*], where *m* and *a* are positive numbers. Quantification factor K_a can be calculated according to (1) and (2).

$$K_a = m / a \tag{1}$$

The discrete numeric value m_i corresponding to the input variable a_i is determined by:

$$m_i = \begin{cases} -m, & k_a.a_i < -m \\ m \quad , & k_a.a_i > m \\ l \quad , & l \le k_a.a_i \le l+1/2 \\ l+1, & l+1/2 \le k_a.a_i \le l+1 \end{cases} \tag{2}$$

l is a positive number less than *m*.

Fuzzy variables $DltU_1$ and $DiffU_1$ shown in Fig. 3 are yielded through the above process.

By computation, the domains of *du* and *du/dt* can be determined as [0, 6] and [-6, 6], respectively. The range of the output variable $DltI_1$ is [0, 6]. Input variables are divided into a range of states defined by fuzzy set, such as *Negative Big* (NB), *Negative Middle* (NM), *Negative Small* (NS), *Zero* (Z), *Positive Small* (PS), *Positive Middle* (PM), and *Positive Big* (PB). The membership functions for *du* and *du/dt* are as shown in Fig. 4.

Based on ac system fault conditions, the effect of *du* and *du/dt* on commutation failure is shown in Section 4. The distribution of membership functions in Fig. 4 is obtained based on the analysis of *du* and *du/dt*. The membership functions of input variables can reflect the influence of different fault resistance on the commutation failure.

According to the fuzzy rule and the analysis of *du* and *du/dt* after faults, the severity of the faults can be divided into different levels. An output fuzzy variable, defined as $DltI_1$, can be derived from two fuzzy variables $DltU_1$ and $DiffU_1$. The corresponding fuzzy control rule base is shown in Table 3.

Table 3 dictates 28 fuzzy rules. For example, when $DltU_1$ is 'PB' and $DiffU_1$ is 'NS', the ac voltage decreases to the lowest point and begins to restore. Since the HVDC system is apt to recover, $DltI_1$ should be the 'PM' to control the voltage reduction quickly.

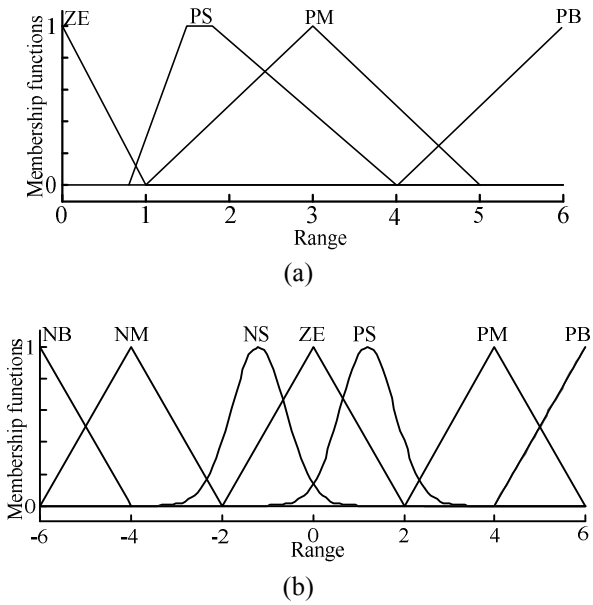

Fig. 4. (a) Membership functions for *du* (b) membership functions for *du/dt*

Table 3. Fuzzy control rule

$DltU_1$ \ $DiffU_1$	PB	PM	PS	ZE	NS	NM	NB
PB	PB	PB	PB	PM	PM	PS	ZE
PM	PB	PB	PB	PS	PS	ZE	ZE
PS	PB	PB	PM	ZE	ZE	ZE	ZE
ZE	ZE	ZE	ZE	ZE	ZE	ZE	ZE

5.2 Defuzzification

Defuzzification is the conversion of $DltI_1$ into a crisp number Z_1*. There are various approaches for defuzzification. In this study, the centroid (centre of mass) method is adopted [21-23]. Z_1* and dI_{f1} are shown as follows:

$$Z_1^* = \frac{\sum_{i=0}^{n} \mu_c(z_i) \cdot z_i}{\sum_{i=0}^{n} \mu_c(z_i)} \quad (3)$$

$$dI_{f1} = k_{u1} \cdot Z_1^* \quad (4)$$

where z_i is the i_{th} component of $DltI_1$, μ_c (z_i) is the membership degree of $DltI_1$ corresponding to z_i, and k_{u1} is the proportional factor.

The membership functions for $DltI_1$ is shown in Fig. 5.

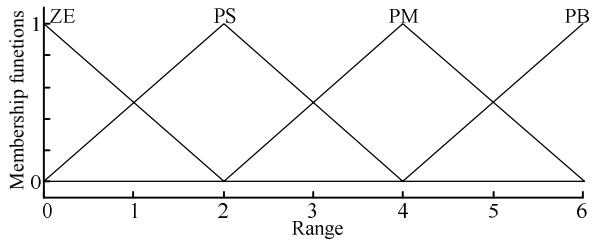

Fig. 5. Membership functions for *DltI1*

The input-output characteristic of the fuzzy controller is calculated offline and is given in Table 4. $DltU_1$ and $DiffU_1$ act as the two input variables through Table 4 to obtain the output value of Z_1*. dI_{f1} can be obtained by multiplying a self-adjusting proportional factor k_{u1} to Z_1*.

A limiter is applied to attain an appropriate output of the prevention controller. The output is denoted as ΔI_1.

The recovery controller is designed by the similar process. ΔI_2 is obtained through fuzzy control. ΔI is the final output of the direct-current fuzzy controller through the selection of ΔI_1 and ΔI_2.

Table 4. Input-output value

$DiffU_1$ \ $DltU_1$	0	1	2	3	4	5	6
-6	0.6469	0.8502	0.6535	0.6469	0.7615	0.7624	0.6469
-5	0.7624	0.8502	0.7624	0.7624	0.7624	1.747	1.747
-4	0.6469	0.8503	0.6536	0.647	0.7616	2.0001	2.0003
-3	0.7624	0.9412	0.825	0.825	0.825	2.0431	2.0435
-2	0.797	2.0006	2.0005	2.0005	2.0005	3.9773	3.9996
-1	0.6498	1.8529	1.8048	1.8329	2.0052	3.9803	3.9999
0	0.6469	2.4189	1.9961	2.1931	2.4489	4.0089	4.0213
1	0.6498	2.9373	3.1376	3.2296	3.0965	4.235	4.4366
2	0.797	3.9994	4.2125	4.2125	5.203	5.203	5.203
3	0.7624	5.0588	5.175	5.175	5.2376	5.2376	5.2376
4	0.6469	5.1497	5.3464	5.353	5.2385	5.2376	5.3531
5	0.7624	5.1498	5.2376	5.2376	5.2376	5.2376	5.2376
6	0.6469	5.1498	5.3465	5.3531	5.2385	5.2376	5.3531

6. Simulation and Validation

In this study, single-phase and three-phase faults are applied to verify the effectiveness of the proposed direct-current fuzzy controller. The verification process is implemented by co-simulation of PSCAD/EMTDC and MATLAB. The test system has been given in Fig. 1.

6.1. PSCAD-MATLAB interface

The direct-current fuzzy controller is a user-defined model. PSCAD/EMTDC can interface with MATLAB/ SIMULINK commands and toolboxes through a special interface. In this paper, the power circuit of the CIGRE HVDC system is modelled in the PSCAD/EMTDC environment. The direct-current fuzzy controller is modelled using MATLAB. By designing and saving a MATLAB program file, denoted as *M*, the HVDC system is interfaced to MATLAB. The interface schematic is shown in Fig. 6.

The input variables collected from the PSCAD/EMTDC simulation are transferred to the fuzzy controller of MATLAB via the data interface. After the direct-current

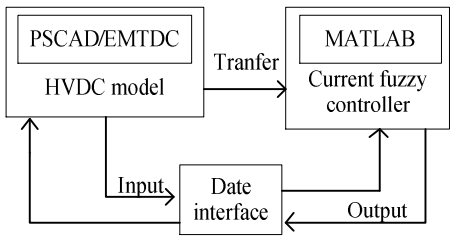

Fig. 6. PSCAD/EMTDC and MATLAB interface schematics

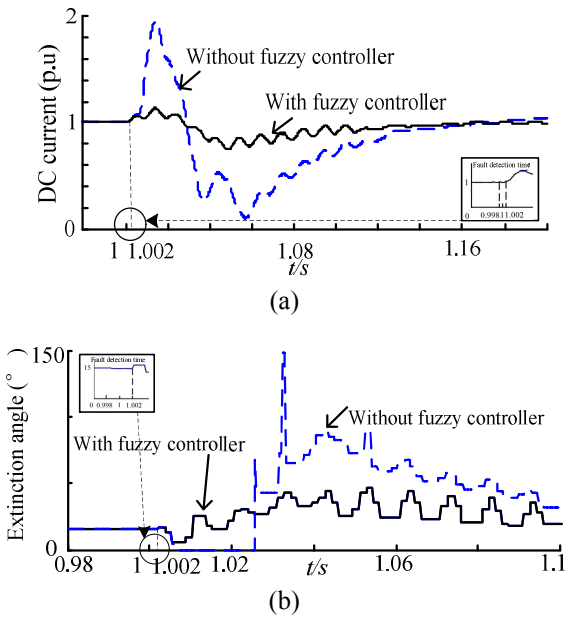

Fig. 7. Single-phase ground fault (a) direct current (b) extinction angle

fuzzy controller, the output variable returns to the PSCAD/EMTDC model to complete the co-simulation.

6.2 Verification with single-phase AC system faults

For single-phase ac system faults at the inverter side, the detailed model of the test system is simulated in PSCAD/EMTDC and MATLAB. The simulation time step is set at 50 μs. The fault is applied at 1 s with fault duration being 0.1 s. The fault detection time is about 2ms. The direct current and the extinction angle with fuzzy control under the single-phase ac faults are presented in Fig. 7.

As shown in Fig. 7(a), the direct current sharply increases to 2.0 p.u. without the fuzzy controller. Subsequently, the direct current decreases with the effect of VDCOL. In Fig. 7(b), the extinction angle drops to 0 at the inverter and results in the occurrence of commutation failures. Thereafter, the extinction angle rises to 150°. After the fault is removed at 1.1 s, the recovery process is initiated. The system returns to stability at 1.16 s.

In the event when the fuzzy controller is applied, the results are different. The prevention controller inhibits the rise and fall of the dc current when the fault occurs. The maximum value of the dc current is below 1.2 p.u. It also attempts to minimize fluctuations in the extinction angle as well as avoids commutation failure. Almost immediately after the fault is removed, the system restores stability. It can be seen that with the fuzzy controller, the direct current, and the extinction angle exhibit relatively faster and more stable recovery.

Therefore, the commutation failure sensitivity is improved under the employment of the direct-current fuzzy controller.

6.3 Verification with three-phase AC system faults

Similar to the conditions of single-phase ac system faults, simulations of three-phase ac system faults are conducted. The simulation results are shown in Fig. 8.

As shown in Fig. 8(a), the direct current has a sudden increase without the proposed fuzzy controller. The maximum direct current reaches 1.9 p.u. In Fig. 8(b), it can be seen that extinction angle decreases rapidly and commutation failure takes place.

After the proposed fuzzy controller is applied in Fig. 8 (a), the maximum direct current is reduced from 1.9 p.u. to 1.17 p.u. The direct current response is smoother than that without the fuzzy controller. In Fig. 8(b), the extinction angle is smaller through adjustment of the fuzzy controller. The commutation failure is avoided during the fault. It can be seen that the recovery controller speeds up the restoration process of direct current and the extinction angle.

Therefore, it is evident that the proposed direct-current fuzzy controller has an obvious effect on prevention and recovery of commutation failure.

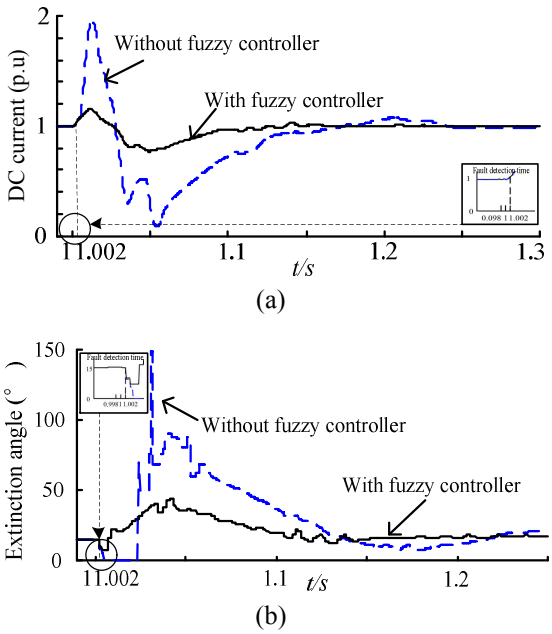

Fig. 8. Three-phase ground fault (a) direct current (b) extinction angle

7. Conclusion

In this study, a direct-current fuzzy controller was designed to mitigate the impact of commutation failures based on the principle of fuzzy control. The current fuzzy controller consists of two parts: prevention controller and recovery controller. Each fuzzy controller is designed based on the analysis of the commutation failure. The efficiency of this direct-current fuzzy controller has been verified through co-simulation based on PSCAD/EMTDC and MATLAB. According to the simulation results, the direct-current fuzzy controller can decrease the frequency of commutation failure in the HVDC system. It can also speed up the recovery of the system from commutation failures. The proposed direct-current fuzzy controller provides an effective measure for prevention of commutation failures in the HVDC systems.

Acknowledgements

The authors would like to thank the anonymous referees for the thoughtful and constructive suggestions that led to a considerable improvement of the paper. This work was supported in part by 'the Fundamental Research Funds for the Central Universities(2018MS087)', in part by 'Colleges and Universities in Hebei Province Science and Technology Research(grant numbers: Z2015041)'.

References

[1] C. V. Thio, J. B. Davies, and K. L. Kent,

"Commutation failures in HVDC transmission systems," *IEEE Trans. Power Del*., vol. 11, no. 2, pp. 946-957, Apr. 1996.

[2] P. Lv, M. Wang, and H. Xu, "Analysis of commutation failure reason in three Gorges-Guangdong HVDC system Echeng station," *Relay* (*China*), vol. 33, no. 18, pp. 75-78, Sep. 2005.

[3] O. U. Kaijian, Ren Zhen, Jing Yong, "Research on commutation failure in HVDC transmission system part 1: commutation failure factors analysis," *Electric Power Automation Equipment*., vol. 23, no. 5, pp. 5-8, 2003.

[4] E. Rahimi, S. Filizadeh, and A.M. Gole, "Commutation failure analysis in HVDC systems using advanced multiple-run methods," *Power Systems Transients* (*PST*), pp. 19-23, 2005.

[5] E. Rahimi, A.M. Gole, J. B. Davies, I. T. Fernando, and K. L. Kent, "Commutation failure in single- and multi-infeed HVDC systems," *IEEE Trans. Power Del*., vol. 26(1), pp. 378-384, 2011.

[6] Z. Wei, Y. Yuan, X. Lei, H. Wang, G. Sun, and Y. Sun, "Direct-current predictive control strategy for inhibiting commutation failure in HVDC converter," *IEEE Trans. Power Syst*., vol. 29, no. 5, pp. 2409-2417, 2014

[7] Sun, Y. Z, et al. "Design a Fuzzy Controller to Minimize the Effect of HVDC Commutation Failure on Power System," *IEEE Transactions on Power Systems*, vol. 23, no. 1, pp. 100-107, 2008.

[8] Bauman, Jennifer, and M. Kazerani. "Commutation Failure Reduction in HVDC Systems Using Adaptive Fuzzy Logic Controller," *IEEE Transactions on Power Systems*, vol. 22, no. 4, pp. 1995-2002, 2007.

[9] Wei, Zhinong, et al. "Direct-Current Predictive Control Strategy for Inhibiting Commutation Failure in HVDC Converter," *IEEE Transactions on Power Systems*, vol. 29, no. 5, pp. 2409-2417, 2014.

[10] T. Machida and Y. Yoshida, "A method to detect the deionization margin angle and to prevent the commutation failure of an inverter for dc transmission," *IEEE Trans. Power App. Syst*., vol. PAS-86, no. 3, pp. 259-262, Mar. 1967

[11] S. Tamai, H. Naitoh, F. Ishiguro, M. Sato, K. Yamaji, and N. Honjo, "Fast and predictive HVDC extinction angle control," *IEEE Trans. Power Syst*., vol. 12, no. 3, pp. 1268-1275, Aug. 1997.

[12] J. Bauman and M. Kazerani, "Commutation failure reduction in HVDC systems using adaptive fuzzy logic controller," *IEEE Trans. Power Syst*., vol. 22, no. 4, pp. 1995-2002, Nov. 2007.

[13] T. Ahn, "Design of the Optimal Self-tuning Fuzzy-Pi Controller for Rectifier Current Control in HVDC System," *Chinese Control Conference IEEE*, pp. 1224-1227, 2006.

[14] M. O. Faruque, Y. Zhang, and V. Dinavahi. "Detailed modeling of CIGRE HVDC benchmark system using PSCAD/EMTDC and PSB/SIMULINK," *IEEE Transactions on Power Delivery*, vol. 21, no. 1, pp. 378-387, 2006.

[15] J. D. Ainsworth, "Proposed benchmark model for study of HVDC controls by simulator or digital computer," in Proc. CIGRE SC-14 Colloq. HVDC With Weak AC Systems, Maidstone, U.K., Sep. 1985.

[16] L. Zhang and L. Dofnas, "A novel method to mitigate commutation failures in HVDC systems," *in Proc. IEEE Power Syst. Technology Conf*, vol. 1, pp. 51-56, Oct. 2002.

[17] F. Nozari, and H. S. Patel. "Power electronics in electric utilities: HVDC power transmission systems," *Proceedings of the IEEE*, vol. 76, no. 4, pp. 495-506, 1988.

[18] J. Choi, G. Hwang, H. T. Kang, and J. H. Park, "Design of Fuzzy Logic Controller for HVDC Using an Adaptive Evolutionary Algorithm," *IEEE International Symposium on Industrial Electronics Proceedings*, vol. 3, pp. 1816-1821, 2001.

[19] M. Szechtman, T. Wess, and C. V. Thio, "First benchmark model for HVDC control studies," *Electra*, vol. 135, no. 4, pp. 54-73, 1991.

[20] L. Zhang and L. Dofnas, "A novel method to mitigate commutation failure in HVDC systems," *IEEE Power System Technology Conf*., vol. 1, pp. 51-56. Oct. 2002.

[21] Z. X. Shao and X. Y. Li, "The HVDC Emergency Power Slaughter Support Adaptive Fuzzy Controller," *Automation of Electric Power Systems. Nanjing*, vol. 26, pp. 1-3, 2002.

[22] H. X. Chen and T. Q. Liu, "An Auxiliary Fuzzy Control for Converter Substation In HVDC System," *Power System Technology. Beijing*, vol. 27, pp. 5-8, 2003.

[23] X. F. Xu, X. Y. Li, Q. Yan, H. C. Liu, and L. Wang, "HVDC Fuzzy Controller to Improve Transient Stability," *Relays*, vol. 32, pp. 16-19, 2004.

Benfeng Gao He received his M.S. and Ph.D. degrees in electrical engineering from North China Electric Power University, China in 2007 and 2011, respectively. Since 2011, he has been with the Department of Electrical Engineering, North China Electric Power University, where he is currently working as associate professor. His research interests include power system sub-synchronous oscillation and control and protection of HVDC system.

Kewei Yuan He received his B.S. degree of Agricultural Electrification and Automation from North China Electric Power University, Baoding, China, in 2016. Since 2016, he has been studying for a M.S. degree in the Department of Electrical Engineering, North China Electric Power University. His research interests include control and protection of HVDC system and wind power system.

Peiyi Dong He received his B.S. and M.S. degrees in electrical engineering from North China Electric Power University, China in 2014 and 2017. Now he is a staff in State Grid Baoding Electric Power Supply Company. His research interests include control and protection of HVDC system and wind power system.

Chao Luo He received the B.S. degree in power system and its automation from Huazhong University of Science and Technology, Wuhan, China, in 2011 and the Ph.D. degree in electrical engineering from North China Electric Power University, Beijing, China, in 2017. Now he is a research assistant in Electric Power Research Institute of China Southern Power Grid. His research interests include analysis and control of subsynchronous oscillation, and power quality analysis.

Shuqiang Zhao He received the B.Sc., M.Sc. and Ph.D. degrees in electrical engineering from North China Electric Power University, China in 1985, 1989 and 1999, respectively. Currently, he is a Professor in the Department of Electrical and Electronic Engineering, North China Electric Power University. His research interests include power system reliability analysis, power system operating and planning.